ACS Catalysis

Research Article

pubs.acs.org/acscatalysis

Hydroaminomethylation of Styrene Catalyzed by Rhodium Complexes Containing Chiral Diphosphine Ligands and Mechanistic Studies: Why Is There a Lack of Asymmetric Induction?

Delphine Crozet,[†,‡] Christos E. Kefalidis,[§] Martine Urrutigoïty,*[,†,‡] Laurent Maron,*[,§] and Philippe Kalck*[,†,‡]

[†]CNRS, Laboratoire de Chimie de Coordination, composante ENSIACET, 4 allée Emile Monso, BP 44362, 31030 Toulouse, Cedex 4, France

[‡]Université de Toulouse UPS-INPT, F-31030 Toulouse, Cedex 4, France

[§]LPCNO, UMR 5215, Université de Toulouse-CNRS, INSA, UPS 135 avenue de Rangueil, 31077 Toulouse Cedex 4, France

Supporting Information

ABSTRACT: Various chiral diphosphine ligands (P−P) have been introduced in the coordination sphere of neutral or cationic rhodium complexes, and the generated species catalyze efficiently the hydroaminomethylation reaction of styrene with piperidine. The diphospholane ligand family is particularly adapted to this tandem reaction leading to the branched amine with good chemo- and regioselectivity. We analyzed in detail the main reasons why the reaction proceeds with no enantioselectivity. Catalytic and HP-NMR experiments reveal the presence of the $[Rh(H)(CO)_2(P-P)]$ species as the resting state. DFT calculations allow us to elucidate the mechanism of the hydrogenation of the branched (*Z*) or (*E*)-enamine. From the $[Rh(H)(CO)(P-P)]$ active species, the coordination of the two enamine isomers, the hydride transfer, the H_2 activation, and then the final reductive elimination follow similar energetic pathways, explaining the lack of enantioselectivity for the present substrates. Analysis of the energy-demanding steps highlights the formation of the active species as crucial for this rate-limiting hydrogenation reaction.

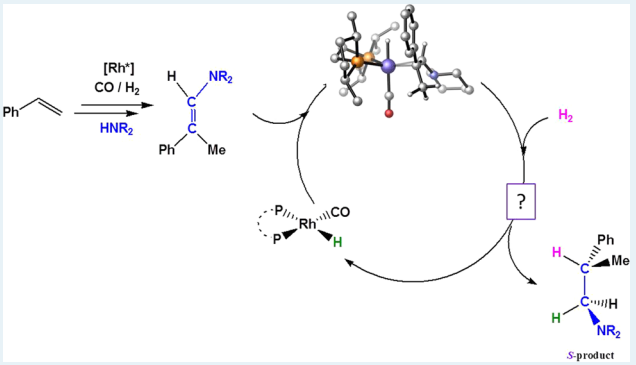

KEYWORDS: *rhodium, hydroaminomethylation, tandem reaction, chiral diphosphine ligands, DFT calculations*

INTRODUCTION

Due to their biological and medicinal properties, amines are of great importance as building blocks or active reactants in fine chemistry.[1,2] To provide an alternative to multistep classical organic synthetic routes, the design of efficient catalysts for their production is of particular interest from an industrial point of view.[3] In that respect, hydroaminomethylation (HAM) is a promising reaction to synthesize amines from alkenes, carbon monoxide, and dihydrogen with a high atom economy. This reaction includes the hydroformylation of an alkene, the condensation of the produced aldehyde with a primary or a secondary amine, and the hydrogenation of the resulting imine or enamine to yield the final amine (Scheme 1). Recent advances in this reaction have been the subject of several reviews.[4]

As HAM is a tandem reaction,[5] it is necessary to carefully design the catalytic system in order to reach high selectivity for the expected amines. The aim is to combine a high activity for both the hydroformylation[6,7] and hydrogenation[8,9] reactions, as well as a high selectivity in the final amines. Rhodium is able to complete both the hydroformylation and the hydrogenation catalytic cycles and is thus often used for HAM. The mechanisms of rhodium-catalyzed hydroformylation[6,7] and hydrogenation[8,9] have been extensively studied, and the active species involved in each catalytic cycle are presumed to be different. Neutral rhodium precursors are often used in hydroformylation, although a few studies are related to cationic rhodium complexes,[10] while cationic precursors are known to generate active hydrogenation catalysts. Thus, the nature of the rhodium precursor to be used is an important issue to consider. Furthermore, to the best of our knowledge, no example of the asymmetric version of this reaction has been reported up to now.[4,11]

The present paper reports on a study on the HAM of styrene with rhodium/chiral diphosphine (P−P) systems. Few studies concern the specific HAM of styrene derivatives. Eilbracht et al.[12] reported the first examples, involving the rhodium precursor $[Rh(\mu\text{-}Cl)(COD)]_2$, under high pressure and

Received: October 11, 2013
Revised: December 16, 2013
Published: December 17, 2013

   dx.doi.org/10.1021/cs400906b | ACS Catal. 2014, 4, 435−447

Scheme 1. Hydroaminomethylation of Alkenes[a]

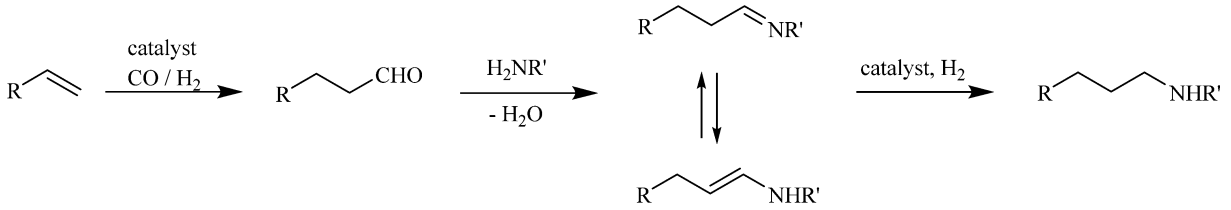

[a]For clarity reasons, only the linear aldehyde isomer has been represented as product of the hydroformylation step.

Scheme 2. Hydroaminomethylation of Styrene with Piperidine

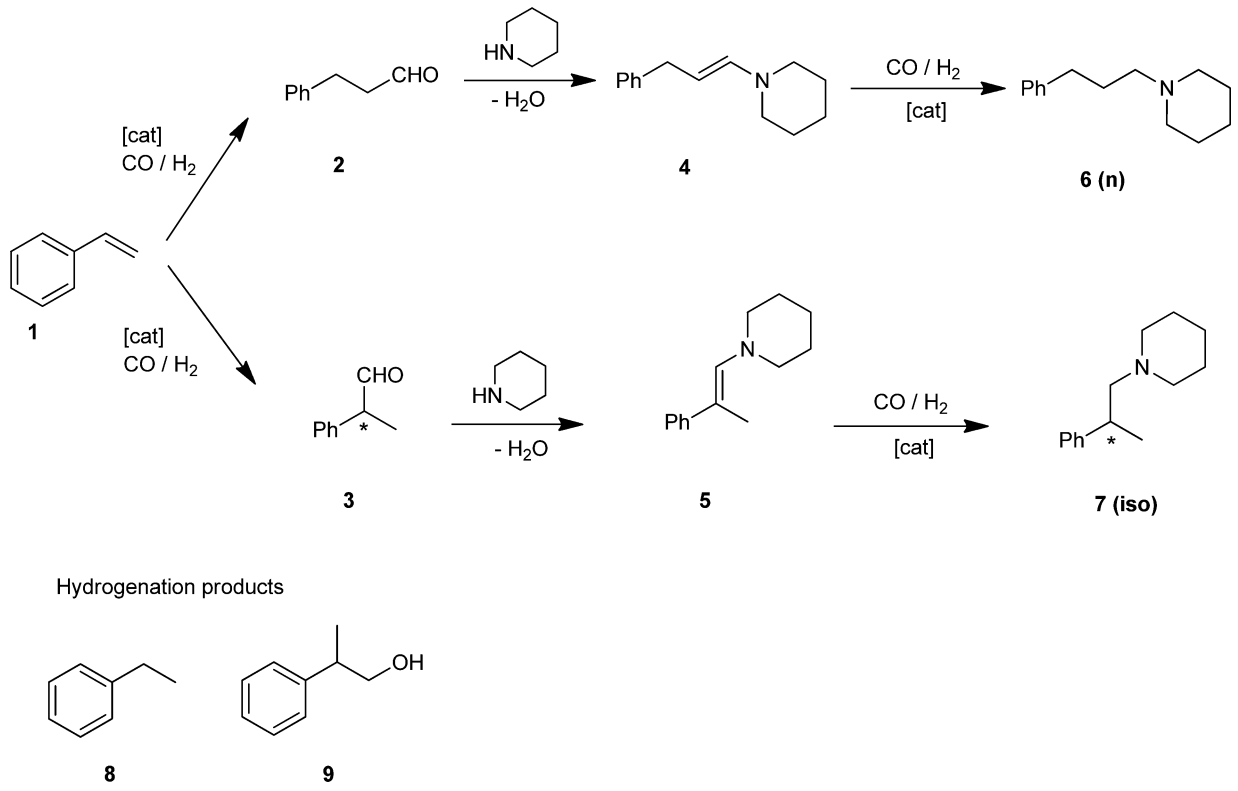

temperature (110 bar, 110 °C) giving for instance with an equivalent mixture of $iPrNH_2$ and $(iPr)_2NH$ an iso/n ratio of 5:1 for a 96% yield. Alper et al. have tested a zwitterionic complex $[Rh^+(COD)(\eta^6\text{-}PhBPh_3)^-]$, under milder conditions (<80 bar, 80 °C) and obtained, still with $iPrNH_2$, a higher 11.5:1 iso/n ratio.[13] A promising rhodium−diphosphine system was developed by Beller et al.[14] that allows the formation of the branched amine with a good iso/n ratio in the presence of aniline. Several diphosphine ligands were used, and the couple $[Rh(COD)_2]BF_4$/dppf (dppf: diphenylphosphinoferrocene) shows the best results in the presence of HBF_4, with a 96% yield and an amine iso/n ratio of 88:12. Recently, introduction of monophosphine ligands containing electron-withdrawing substituents, particularly the tris(3,4,5-trifluorophenyl)-phosphine, led Clarke et al. to obtain 92% of the branched amine.[15]

In line with preliminary studies,[16,17] we investigated the influence of the nature of the rhodium precursor, starting either from the cationic rhodium preformed precursors $[Rh(COD)(P-P)]^+$ and $[Rh(CO)_2(P-P)]^+$ or from the neutral $[Rh(acac)(CO)_2]$/diphosphine system. Combination of catalytic experiments and high-pressure NMR studies allowed us to identify some key species formed during the reaction. DFT calculations were also carried out in order to get further insights into the mechanism of the reaction, particularly to explain the absence of any enantioselectivity.

RESULTS AND DISCUSSION

Catalysis. In order to develop the asymmetric version of the reaction, we decided to investigate the HAM of styrene (Scheme 2), which provides a chiral branched amine. We chose to use piperidine as the secondary amine coreactant to avoid the imine/enamine isomerization reaction (Scheme 1).

First, we analyzed from the literature the separate performances of various rhodium−phosphine catalytic systems either for hydroformylation or for hydrogenation of functionalized −C═C− bonds. The ligand donor/acceptor properties required seem to be opposite to get a good activity for each step of the tandem process. It is well-known that the more π-acceptor the phosphine ligand is, the more efficient is the hydroformylation reaction.[6,18,19] In this case, the electron-withdrawing character of the ligand plays a crucial role for the system activity, since the alkene double bond coordination as well as the migratory CO insertion are favored by an electrophilic metal center. On the other hand, the necessary

dx.doi.org/10.1021/cs400906b | ACS Catal. 2014, 4, 435−447

σ-donor properties of the diphosphine ligand involved in the carbon−carbon double bond hydrogenation are often highlighted.[20] An electron-rich diphosphine ligand favors the oxidative addition of H_2, or the migratory insertion step leading to the alkyl−rhodium species, which are often described as the rate-determining steps.[21] However, the exact influence of the ligands on the whole HAM process remains difficult to rationalize. Kinetics of each elementary step of a catalytic cycle depends not only on a complex equilibrium between the ligands σ-donor and π-acceptor properties but also on the nature of the unsaturated substrate involved.

As relative rates of the successive reactions are of crucial importance, we decided to choose efficient ligands for hydroformylation. This catalytic reaction has to operate very fast, in order to avoid competitive reactions such as alkene hydrogenation. The enamine **5** (Scheme 2), obtained from the branched aldehyde is conjugated and is expected to be more difficult to hydrogenate with regard to the linear enamine **4**. Furthermore, in this case, the key step for enantioselectivity is the hydrogenation of the enamine **5**, which produces the asymmetric center. The chirality of the carbon atom of the aldehyde **3** is lost during the condensation reaction of piperidine with the branched aldehyde but leads to the formation of the prochiral double −C═C−N− bond (Scheme 2). The design of the catalyst requires taking these points into account. Thus, we identified some promising diphosphine ligands (Scheme 3) for this tandem reaction,[22,23] especially the phospholane-type ligands[24] such as the Ph-BPE[25] and Duphos-type ligands[26,27] or the P-chirogenic ligands such as Tangphos,[28] Duanphos,[29] and Binapine,[30] which provide high enantioselectivities[31] for both reactions. Other diphosphine ligands known to be efficient in hydrogenation but with σ-donor and π-acceptor properties adapted to hydroformylation requirements can be of interest in this reaction as well. First, atropoisomeric ligands[32] with a biphenyl backbone, such as MeO-BIPHEP[33] and Synphos,[34] (ligand kindly provided by Pr Genêt J.-P., from the Laboratoire Charles Friedel at Chimie Paris Tech ENSCP) or as the binaphtyl Tol-BINAP ligand were tested. The Josiphos-type ligand (*R*)-(*S*)-PPF-PXyl$_2$[35] and the ferrocenyl ligand Me-Ferrocelane were considered as well.

Comparison between Cationic and Neutral Rhodium Systems. The importance of the nature (cationic or neutral) of the rhodium precursor used in the HAM reaction was pointed out in recent studies. Beller et al. first proposed the use of a cationic rhodium precursor in combination with phosphine ligands, in order to favor the formation of cationic species active in hydrogenation.[36] Similar observations were made by Vogt et al.[37] In a study on the oct-1-ene HAM in ionic liquids, this research group compared the activity of systems with $[Rh(COD)_2]BF_4$ and $[Rh(COD)_2]BF_4/[Rh(acac)(CO)_2]$, with SulfoXantphos as the ligand.[38] The mixed cationic/neutral system gave a higher rate of oct-1-ene conversion than the only $[Rh(COD)_2]BF_4$ precursor. Whereas a significant difference between the cationic and cationic/neutral system is observed during the early stage of the reaction (4h), the product distribution is similar at the end (18h). The authors noted that, as expected, the hydroformylation activity was improved since the $[Rh(acac)(CO)_2]$ precursor is known to easily generate the active hydroformylation species.

Taking into account these recent results, we prepared some cationic rhodium precursors, typically $[Rh(COD)\{(R,R)$-Ph-BPE$\}]BF_4$ (COD = 1,5-biscyclooctadiene) or $[Rh(CO)_2\{(R,R)$-Ph-BPE$\}]BF_4$, with Ph-BPE **L1**, which was foreseen as part of the most efficient ligands. Then, we compared them with the neutral $[Rh(acac)(CO)_2]$/Ph-BPE system for styrene/piperidine HAM (see SI, Tables S1 and S2). Former HAM studies with styrene and piperidine led us to select 90 °C, 30 bar CO/H_2 (1:2) as suitable temperature and CO/H_2 pressure, which are close to those classically used in this reaction.[36b] As expected, an increase of either the temperature or the H_2 partial pressure favors the enamine hydrogenation reaction and allows to get higher selectivity in amines, but it also influences the regioselectivty, with lower iso/n ratios (see SI, Tables S1 and S2). In the HAM of alkenes such as oct-1-ene (see SI, Table S3) or α-methylstyrene with piperidine (see SI, Table S4), we also observed that for long reaction times, final product distribution was similar for both cationic and neutral systems with the Ph-BPE ligand. For these two latter alkenes, the hydrogenation step is not rate-determining, since the enamine intermediates are not present in the reaction mixture. In the case of styrene, however, the rate-determining step is the hydrogenation of the conjugated enamine **5**, and the influence of the cationic or neutral precursor can be precisely evaluated. The three following systems were thus investigated: the neutral precursor $[Rh(acac)(CO)_2]$ combined to Ph-BPE, the cationic precursor $[Rh(CO)_2\{(R,R)$-Ph-BPE$\}]BF_4$, and a mixture of the two (Table 1).

Scheme 3. Chiral Diphospholane Ligands Examined in the Present Study

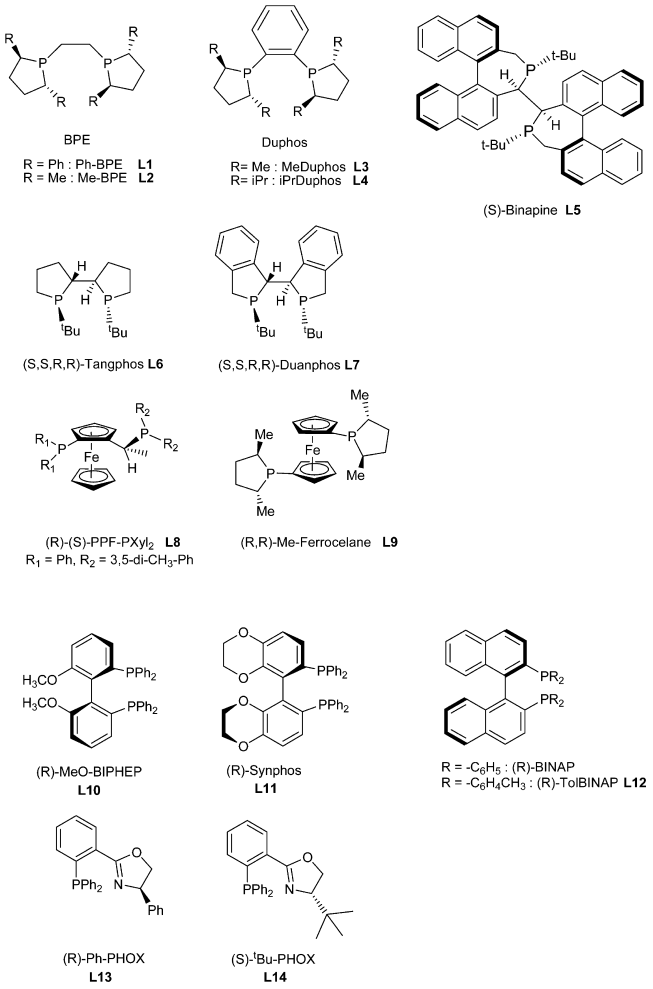

dx.doi.org/10.1021/cs400906b | ACS Catal. 2014, 4, 435−447

Table 1. Hydroaminomethylation of Styrene with Piperidine Catalyzed by Rhodium Cationic and Neutral Systems

			product selectivity (%)			
	rhodium precursor	conversion of styrene (%)	amines (iso/n)	branched aldehyde	branched enamine	hydrogenation products[c]
1	$[Rh(CO)_2\{(R,R)\text{-Ph-BPE}\}]BF_4$	100	19 (64:36)	12	69	traces
2[b]	$[Rh(acac)(CO)_2]/(R,R)$-Ph-BPE + $[Rh(CO)_2\{(R,R)\text{-Ph-BPE}\}]BF_4$	100	30 (56:44)	14	54	traces
3	$[Rh(acac)(CO)_2]/(R,R)$-Ph-BPE	100	48 (64:36)	8	40	2.5

[a]Conditions: styrene (10 mmol), piperidine (10 mmol); amine/alkene =1; 90 °C; 30 bar CO/H_2; 45 mL THF; 7h; S/Rh = 500; L/Rh = 1.2. [b]S/Rh^+ = 1000; S/Rh = 1000. [c]Ethylbenzene and 2-phenyl-propan-1-ol

Table 2. Hydroaminomethylation of Styrene with Piperidine Catalyzed by $[Rh(acac)(CO)_2]$−Chiral Diphosphine Systems

			product selectivity (%)				
	ligand combined with $[Rh(acac)(CO)_2]$	conversion of styrene (%)	amines (iso/n)	branched aldehyde	branched enamine	hydrogenation products[e]	% ee
1		96	89 (66:34)	9	1	0.3	0
2	(R,R)-Ph-BPE **L1**	100	48 (64: 36)	8	40	2.5	0
3	(R,R)-Ph-BPE **L1**	100[b]	62 (74:27)	1	36	1	0
4	(R,R)-Me-Duphos **L3**	91	42 (62:38)	7	48	2.8	0
5	(R,R)-iPr-Duphos **L4**	>99[c]	86 (70:30)	0.5	2	7.4	0
6	(S)-Binapine **L5**	93	88 (75:25)	9	1		0
7	(S,S,R,R)-Tangphos **L6**	91	74 (75:25)	8	14	2.3	0
8	(R,R,S,S)-Duanphos **L7**	90	87 (73:27)	7	6	0.5	0
9	(R)-(S)-PPF-$PXyl_2$ **L8**	85	29 (46:53)	6	62[d]		0
10	(R,R)-Me-Ferrocelane **L9**	>99	42 (48:52)	9.5	47	traces	0
11	(R)-MeO-BIPHEP **L10**	50	7 (43:56)	2	86[d]	0.5	0
12	(R)-Synphos **L11**	43	3 (32:68)	11	80[d]	traces	0
13	(R)-Tol-BINAP **L12**	65	5 (41:59)	4	85	4	0

[a]Conditions: $[Rh(acac)(CO)_2]$, styrene (10 mmol), piperidine (10 mmol), S/Rh = 500, ligand/Rh = 1.2, 90 °C, 30 bar CO/H_2 (1:2), 45 mL THF, 7h. [b]24 h. [c]19 h. [d]Trace amounts of the linear isomer. [e]Ethylbenzene and 2-phenyl-propan-1-ol.

Since styrene conversion is complete after 2 h of reaction, the reported selectivities reflect the hydrogenation activity of the system. The $\{[Rh(acac)(CO)_2]/(R,R)$-Ph-BPE$\}$ system is the most efficient.

The regioselectivity of the hydroformylation reaction and the final selectivity in amines are independently ruled by the different reaction parameters, and these latter can have some opposing effects (see SI, Figure S1 and Figure S2). The presence of both carbon monoxide and amine in the reaction mixture can influence the formation of the active species inherent to the hydrogenation and hydroformylation reactions and also the rate of each catalytic step. The presence of CO slows down the hydrogenation step, particularly for the branched enamine **5** (see SI, Figure S1a). The presence of a large excess of amine (compared to rhodium) slows down the rate of the hydroformylation and influences the regioselectivity of the reaction, regardless of the cationic or neutral rhodium precursor used (see SI, Figure S2). Finally, it is known that high temperature or H_2 partial pressure favors the formation of the linear aldehyde instead of the branched isomer of interest in our case, but on the other hand, it favors the enamine hydrogenation step and also higher amine selectivity.[6] These antinomic effects are relevant to this tandem reaction and must be adapted to each couple of substrates and to each peculiar objective.

Performances of Rhodium−Chiral Diphosphines Systems. Thanks to these preliminary results, the performances of a series of diphosphine ligands were investigated with the $\{[Rh(acac)(CO)_2]$/diphosphine$\}$ system (Table 2). The results are very similar for ligands belonging to the same family (Figure 1). The biaryl ligands MeO-BIPHEP **L10**, Synphos **L11** and Tol-BINAP **L12** (entries 11, 12, and 13) did not prove to be efficient for HAM, the styrene conversion being limited to ≈40−50%, with very low amine selectivity (<8%). The hydroformylation step does occur but remains slow. The enamines are the major products so that their hydrogenation is limitative. The Josiphos type ligand (R)-(S)-PPF-$PXyl_2$ **L8** reveals to be more efficient than the biaryl ones, with a 29% amine selectivity as well as a higher hydroformylation rate, leading to 85% conversion and no other hydrogenation product detection (entry 9). The selectivity in amines and enamines obtained with the diphospholanes Ph-BPE **L1**, Me-Duphos **L3**, and Me-Ferrocelane **L9** ligands are about 40−50% after a 7 h reaction time. Hydroformylation of styrene is almost complete. Experiments carried out with the Ph-BPE and iPr-Duphos ligands (entries 2, 3, and 5) show that the amine selectivity increases with reaction time, consistent with a rate-limiting hydrogenation step.

The best results in terms of selectivity were obtained with the P-chirogenic Tangphos, Duanphos, and Binapine ligands (entries 6, 7, and 8), with a conversion of styrene around 90% and amine selectivity from 74 to 88%. (Figure 1b). This result is in phase with the performances of these ligands in hydrogenation.[31] In all cases, the final iso/n amine ratio is affected because of the presence of amounts of non-hydrogenated branched enamine (Table 2). Surprisingly, no enantiomeric excess was obtained regardless of the $[Rh(acac)(CO)_2]$/diphosphine system used (monitoring of the reaction

dx.doi.org/10.1021/cs400906b | ACS Catal. 2014, 4, 435−447

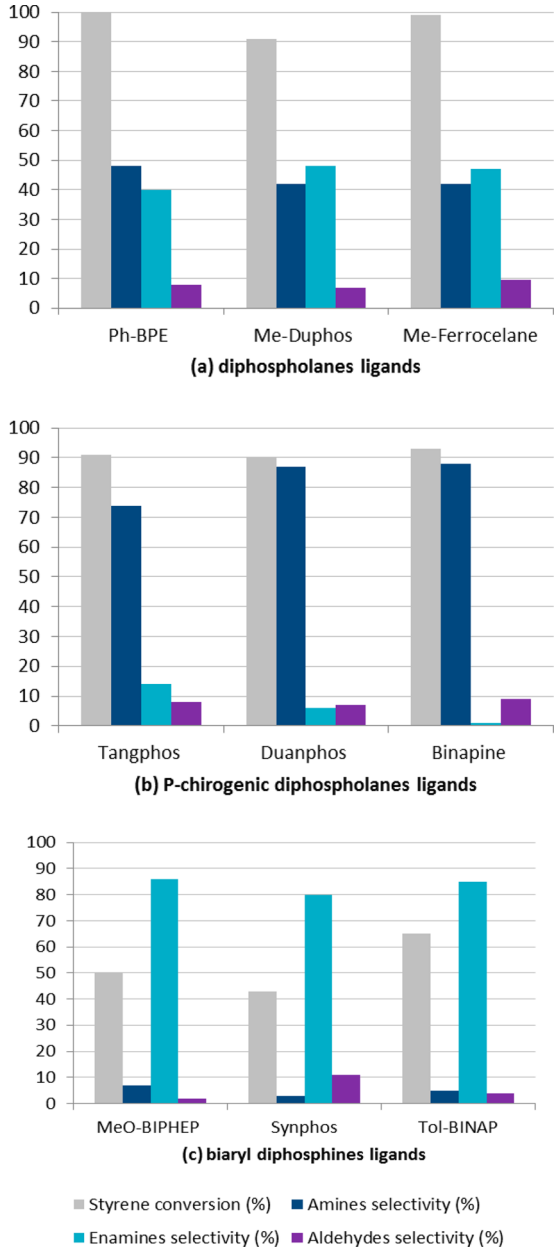

Figure 1. Conversions and selectivity obtained with rhodium complexes bearing (a) phospholane ligands, (b) P-chirogenic phospholane ligands, (c) biaryl diphosphine ligands.

and analysis at the end of the reaction by chiral gas chromatography).

In order to check if it could arise from a problem during the formation of the postulated starting precursor $[RhH(CO)_2(P-P)]$, the latter was prepared in situ before the introduction of the substrates (details are given in the Experimental Section. For both HAM and reductive amination reactions, no enantiomeric excess was obtained with either the (*R*,*R*)-Ph-BPE or (*S*)-Binapine ligands. Additionally, the use of preformed cationic precursors $[Rh(COD)\{(R,R)\text{-Ph-BPE}\}]BF_4$, $[Rh(COD)(R,R,S,S)\text{-Duanphos})]BF_4$, $[Rh(COD)((S,S,R,R)\text{-Tangphos})]BF_4$ does not result in any enantiomeric excess (see SI, Table S5). The influence of some parameters was investigated in an attempt to get better insights. Thus, changing the counterion BF_4^- to NTf_2^- in the cationic complex $[Rh(COD)\{(R,R)\text{-Ph-BPE}\}]^+$ did not show any significant difference in the final selectivity. Addition of molecular sieves to favor the displacement of the enamine formation equilibrium toward the aldehyde consumption by water adsorption, allows a selectivity in amines up to 62% with $[Rh(COD)\{(R,R)\text{-Ph-BPE}\}]BF_4$. In a toluene/isopropanol solvent system, higher amounts of hydrogenation products **8** and **9** were observed, still with no enhancement of the amine enantioselectivity (see SI, Table S5).

These catalytic experiments demonstrate that the hydrogenation of the enamines is the rate-determining step, especially for the branched enamine isomer. The diphosphine ligand plays a crucial role in controlling the selectivity of the reaction. The neutral rhodium precursor is more efficient than the cationic one, even if cationic complexes are known to be more active for hydrogenation reactions. These results point to that in HAM, the presence of CO and amine dramatically influences the course of the reaction and changes the behavior of species classically observed for both the hydroformylation and the hydrogenation reactions. However, whatever the conditions investigated, no enantiomeric excess could be obtained.

Different explanations can be proposed to rationalize the absence of enantiomeric excess: (i) a nonsuitable metal−ligand association leading to an active species with no enantiodiscrimination, (ii) a racemization of the final product due to the reaction conditions, or (iii) the nature of the hydrogenated intermediates, since the enantioselection occurs during the hydrogenation reaction. High-pressure NMR experiments were performed to determine the most likely active species of the hydrogenation reaction under the HAM conditions (CO/H_2 pressure, amine).

High-Pressure NMR Experiments. First, the HAM reaction was performed in THF-d^8 with $[Rh(CO)_2\{(R,R)\text{-Ph-BPE}\}]BF_4$ in order to analyze the crude mixture during the course of the reaction. ^1H NMR analyses at different reaction times as well as HP-NMR experiments have shown the presence of both (*Z*) and (*E*) isomers of the 1-(2-phenylprop-1-1-enyl)piperidine **5**. These latter are characterized in ^1H NMR by the signal of their ethylenic proton -PhMe-C=C**H**(NC_5H_{10}) at δ = 5.85 ppm for the (*Z*)-enamine and δ = 6.14 ppm for the (*E*)-enamine. The two isomers are continuously present in the reaction mixture (see SI, Figures S3 and S4). The condensation reaction between the linear aldehyde and piperidine occurs very fast since only traces of linear aldehyde can be detected. In the case of the reaction between the branched aldehyde and piperidine, the (*Z*)-enamine is formed faster than the (*E*)-one. The proportion of the (*E*)-enamine progressively increases along the reaction with time, temperature, and with the (Z)-enamine isomerization until being the major enamine product. The simultaneous presence of the (*E*)- and (*Z*)-enamine can be of crucial influence on the enantioselectivity results or on the hydrogenation activity during the reaction, since one of the two isomers can be more quickly hydrogenated. It is well-known that due to the steric hindrance induced at the metal center, some diphosphine ligands can be selective for one isomer.[39] According to the active species involved in the hydrogenation catalytic cycle, the coordination of the −C=C−N− double bond can be favored for one of them due to steric hindrance, influencing both the hydrogenation rate and the enantioselectivity.

In order to get a first insight into the rhodium species involved in the reaction, high-pressure ^{31}P and ^1H NMR

dx.doi.org/10.1021/cs400906b | *ACS Catal.* 2014, 4, 435−447

Scheme 4. Rhodium Complexes Detected during HP-NMR Experiments

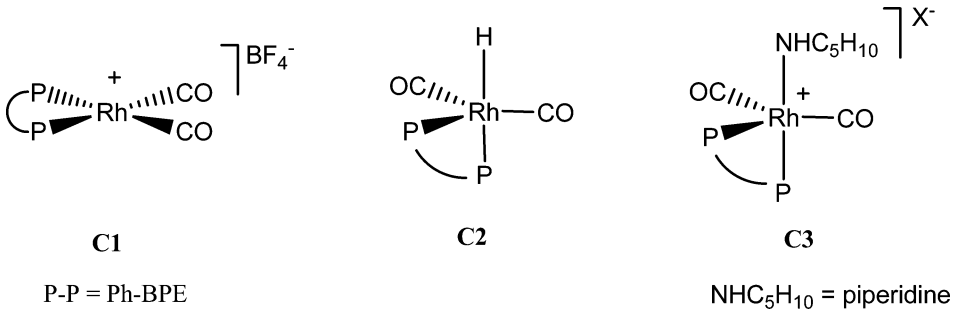

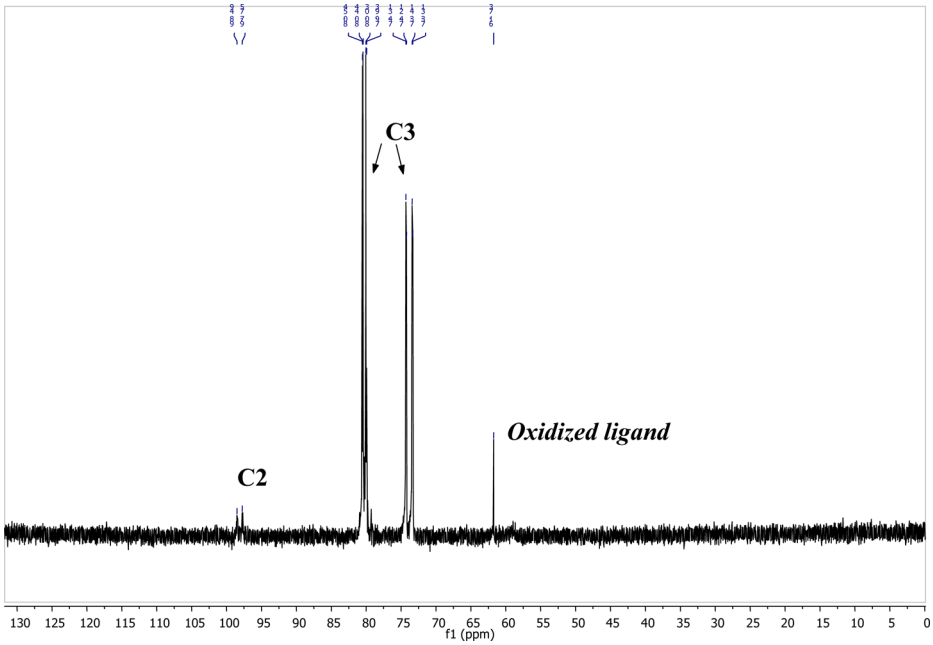

Figure 2. ^{31}P NMR of the solution of C1 with 100 equiv piperidine and styrene after 5 min under 30 bar CO/H_2 (1:2), in THF-d^8, at 298K.

experiments were performed under conditions close to those of catalysis (30 bar CO/H_2 (1:2), styrene/Rh = 100, piperidine/Rh = 100) with both $[Rh(acac)(CO)_2]$/Ph-BPE, and $[Rh(CO)_2\{(R,R)\text{-Ph-BPE}\}]BF_4$ systems.

Previous studies[16,17] have shown that under these conditions, the cationic complex $[Rh(CO)_2\{(R,R)\text{-Ph-BPE}\}]BF_4$ **C1** reacts immediately to give small amounts of the neutral monohydride species $[RhH(CO)_2\{(R,R)\text{-Ph-BPE}\}]$ **C2** and the amino pentacoordinated complex $[Rh(NHC_5H_{10})(CO)_2\{(R,R)\text{-Ph-BPE}\}]BF_4$ **C3** formed due to the large excess of amine (Scheme 4 and Figure 2).

^{31}P NMR experiments performed from $[Rh(acac)(CO)_2]$ without syngas pressure (Figure 3a) showed $[Rh(acac)\{(R,R)\text{-Ph-BPE}\}]$ **C4** as the major species,[16] characterized by a doublet at 105.7 ppm ($^1J_{Rh-P}$ = 201 Hz) as well as the presence of the cationic complex $[Rh(CO)_2(NHC_5H_{10})\{(R,R)\text{-Ph-BPE}\}]^+$ **C3**. In this case, the acetylacetonato entity plays the role of counteranion. The formation of rhodium cationic species with diphosphine ligands and $acac^-$ as counterion was already described.[40,41] Attempts to isolate the complex $[Rh(CO)_2(NHC_5H_{10})\{(R,R)\text{-Ph-BPE}\}]acac$ **C3** were unsuccessful, since the stabilization of the rhodium cation by $acac^-$ is somewhat less efficient than by BF_4^-.[16] ^{31}P NMR analyses under 30 bar CO/H_2 (1:2) revealed after 15 min the presence of the doublet of the monohydride species **C2** at 97.9 ppm due to a fast exchange phenomenon of the two phosphorus atoms on the NMR time scale and the two doublet of doublets of **C3** at 73.7 and 80.2 ppm.[16] Complex **C4** is still observed, but it rapidly disappears to lead to **C2**. The signals of some other unidentified species, probably related to the fast reactivity with styrene under HP-NMR conditions, were also observed (Figure 3b). Studies are under investigation in order to assign the signals of these minor species.

These high-pressure NMR experiments showed that whatever the precursor, two common species are formed at the very beginning of the reaction (30 bar CO/H_2 (1:2), 298K): the monohydride complex **C2** and the pentacoordinated cationic complex **C3** in different proportions. Complexes **C2** and **C3** were obtained with a 40:60 ratio starting from the $[Rh(acac)(CO)_2]$ precursor and with a 5:95 ratio from $[Rh(CO)_2\{(R,R)\text{-Ph-BPE}\}]BF_4$ (Figure 4). We believe that the difference of activity between the cationic and neutral systems could be related to their ability to generate the $[RhH(CO)_2(P-P)]$ species, which appears as the main key species of the HAM reaction.

This hypothesis is reinforced by results of a reported study describing the use of the $[RhH(CO)_2(Chiraphos)]$ complex in the enone hydrogenation reaction.[42] In this study, the complex is prepared under hydroformylation conditions ($[Rh(acac)(CO)_2]$/Chiraphos, 80 bar CO/H_2, 2h, 60 °C) before

dx.doi.org/10.1021/cs400906b | ACS Catal. 2014, 4, 435−447

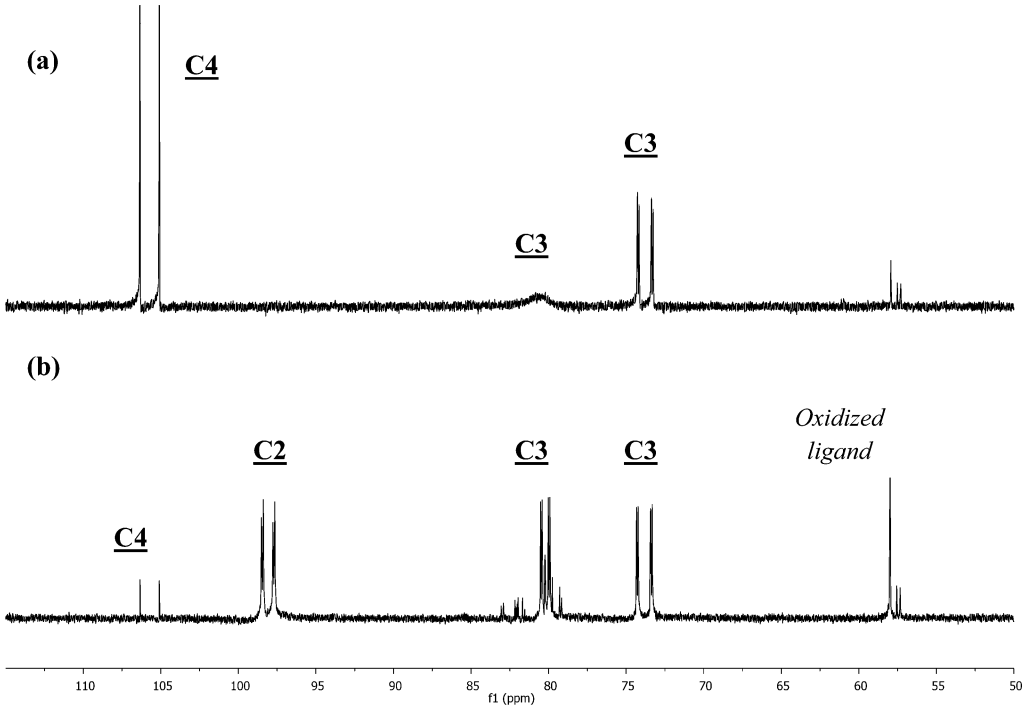

Figure 3. ^{31}P NMR spectra of a solution of $[Rh(acac)(CO)_2]$/(*R*,*R*)-Ph-BPE in the presence of piperidine (100 equiv) and styrene (100 equiv) in THF-d^8 at 298K (a) without pressure, under argon atmosphere (b) under 30 bar CO/H_2 (1:2) after 15 min.

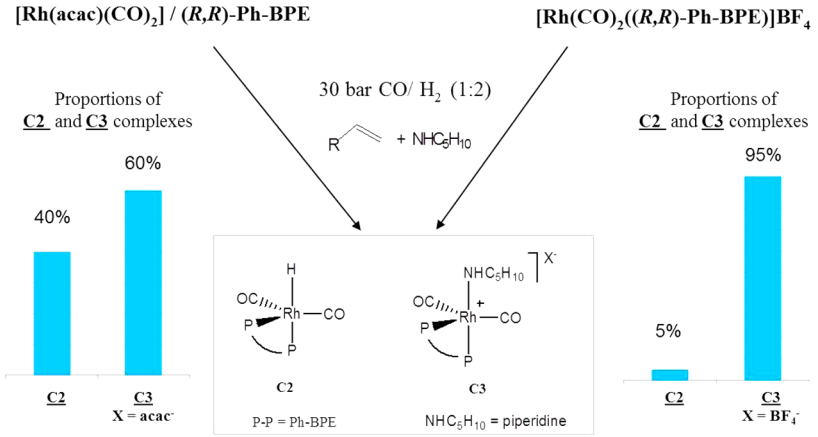

Figure 4. Rhodium species observed after 15 min under 30 bar CO/H_2 (1:2), at 25 °C, THF-d^8, in the presence of piperidine (100 equiv) and styrene (100 equiv).

introducing the enone and performing its hydrogenation under 80 bar H_2. The key point is that under similar preformation conditions, the $[Rh(COD)_2]BF_4$/Chiraphos system did not catalyze the hydrogenation of the enone substrate, whereas the $[Rh(acac)(CO)_2]$/Chiraphos system was active. Our observations are consistent with these results. In the case of the cationic system, the difference between this latter study and our own work is the presence of the amine in the mixture. We recently showed that under CO/H_2 pressure, $[Rh(COD)_2]BF_4$/P−P or $[Rh(COD)(P-P)]BF_4$ lead only to the formation of the cationic complex $[Rh(CO)_2(P-P)]^+$, and that the presence of a base such as THF or an amine allows us to generate the $[RhH(CO)_2(P-P)]$ species.[16]

All these observations led us to identifiy the $[RhH(CO)_2(P-P)]$ complex **C2** as the most likely precursor for the active species of the hydrogenation, so that it was chosen as the starting complex in the following DFT studies performed in order to get insight on the mechanism of the reaction and to explain the absence of enantioselectivity.

Computational Study. The purpose of the computational study is to give insights on two critical points of the present experimental work. First, we investigated the relative high temperature needed in order for the catalysis to proceed as well as the observed lack of enantioselectivity of the hydrogenation step. In this respect, free energy profiles were computed using DFT for the hydrogenation of the 1-(2-phenylprop-1-enyl)-piperidine (**5**). The rhodium complexes were modeled using Me-BPE as ligand rather than Ph-BPE. This modeling was shown to be adequate in a previous study involving similar species[16] as the computed free energies were found to be consistent with the two systems (full experimental and reduced one).

First, the dissociation of one carbonyl group from the initial complex $[RhH(CO)_2\{(R,R)$-Me-BPE$\}]$, **E1**, yields the "active

dx.doi.org/10.1021/cs400906b | *ACS Catal.* 2014, 4, 435−447

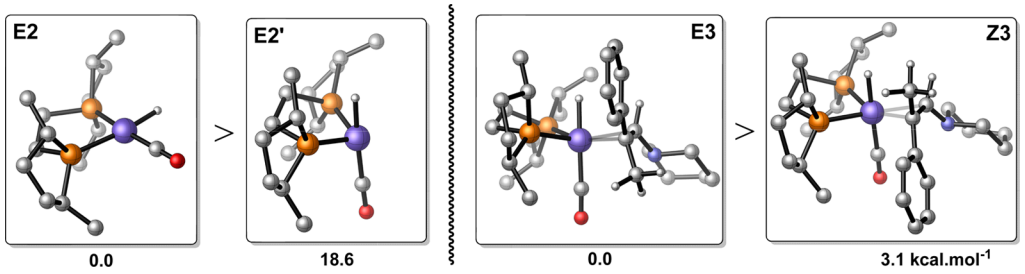

Figure 5. Optimized geometries and comparisons between Gibbs free energies for the isomers E2 vs E2′ and E3 vs Z3. Most of the hydrogen atoms were omitted for clarity.

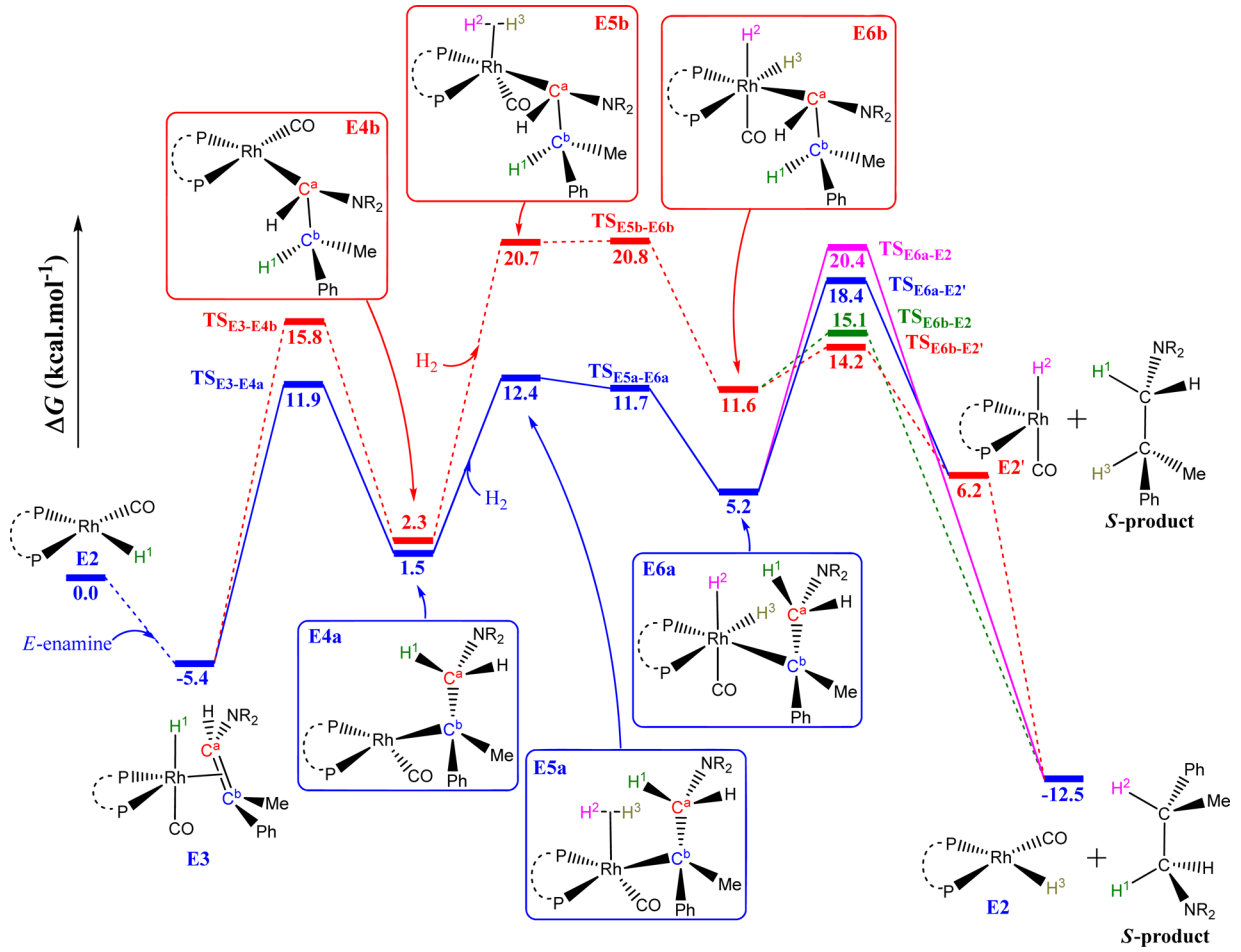

Figure 6. Possible Gibbs free energy (kcal·mol^{-1}) profiles for the hydrogenation of (*E*)-enamine catalyzed by E2.

catalyst" [RhH(CO){(*R*,*R*)-Me-BPE}] **E2**, which adopts a square planar geometry (Figure 5). The relatively high endoergicity of this dissociation (18.7 kcal·mol^{-1}), is the result of the loss of a strong interaction between the metal and the good σ-donor and π-acceptor CO ligand. Another isomer, **E2′**, was also found as local minimum on the potential energy surface but 18.6 kcal.mol^{-1} higher in energy than the global minimum **E2**. The former adopts a distorted trigonal pyramidal geometry, as is shown in Figure 5. However, the estimated high energy difference between **E2** and **E2′** indicates that the isomerization **E2** → **E2′** is thermodynamically unfavorable. The formation of the intermediate **E2** (already proposed in the literature)[6] is thus thermodynamically disfavored at room temperature. This correlates with the high temperature needed for the reaction to proceed so that one key step for hydrogenation is already the formation of the active species. Therefore, **E1** can be considered as a dormant species and could represent the catalyst resting state.

The unsaturated 16e$^-$ monomeric species **E2** could react with the enamine to yield the catalytically competent 18e$^-$ species formulated as [Rh(H)(CO){(*R*,*R*)-Me-BPE}(η^2-enamine)]. Considering the stereochemistry of the full rhodium–enamine complexes along with the chirality induced by the diphosphine ligand, it results in the hypothetical existence of four different isomers for both (*E*)- and (*Z*)-enamine (see SI, Figure S5). For the former, the most stable complex is **E3** with the enamine occupying the equatorial position of the distorted trigonal bipyramid along with the BPE ligand, while the remaining axial positions are occupied by a carbonyl and a

dx.doi.org/10.1021/cs400906b | ACS Catal. 2014, 4, 435−447

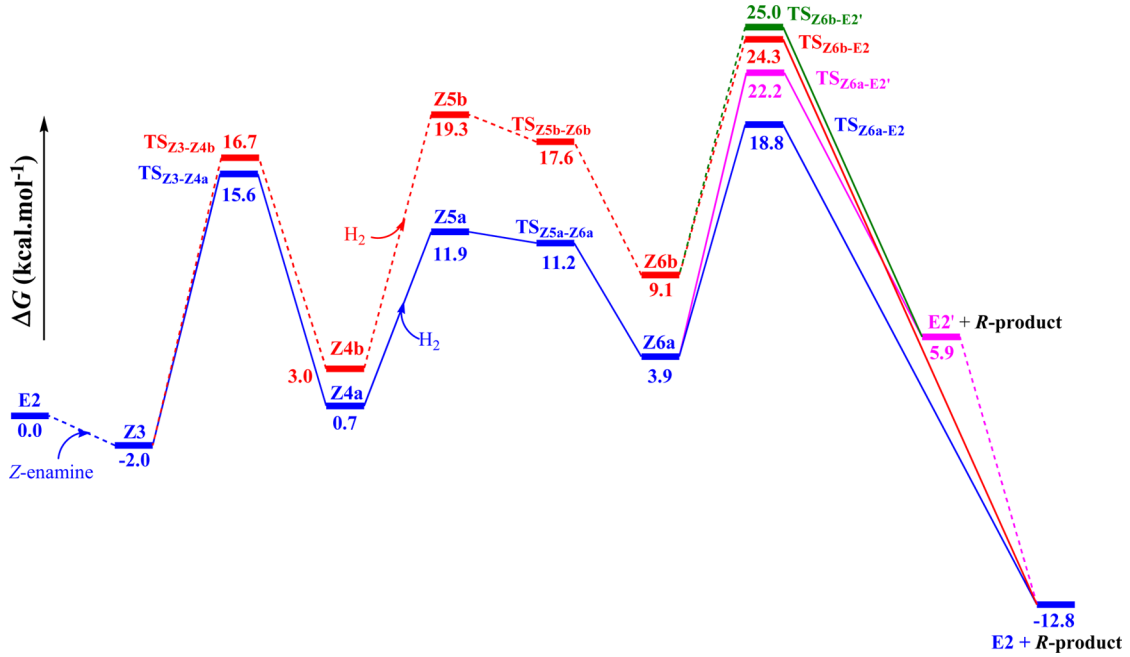

Figure 7. Possible Gibbs free energy (kcal·mol^{-1}) profiles for the hydrogenation of (*Z*)-enamine catalyzed by E2.

hydride. The same also holds true for complex **Z3** for the rhodium−(*Z*)-enamine complex (Figure 5).

Apart from these configurations, we also examined the other possibility of coordination isomers. For instance, a distorted tetrahedral geometry is possible. However, energetically all the other configurations lie above the most stable intermediate **E3** or **Z3** respectively (see SI, Figure S5). It should be noticed that profiles involving slightly higher in energy intermediates than **E3** and **Z3** were computed and were found not to be kinetically competitive with those described hereafter (see SI). Thus, the latter complexes (**E3** and **Z3**) will be the references throughout this study.

All the considered free energy pathways for the hydrogenation of (*E*)-enamine catalyzed by the **E2** isomer are depicted schematically in Figure 6.

Coordination of the enamine to the catalytically active complex **E2** results in the formation of intermediate **E3** and is an exoergic process (−5.4 kcal·mol^{-1}). From intermediate **E3**, insertion of the enamine to Rh−H bond can be achieved through two different cyclic four-membered transition states, namely, $\mathbf{TS_{E3\text{-}E4a}}$ and $\mathbf{TS_{E3\text{-}E4b}}$, yielding intermediate **E4a** and **E4b**, respectively. The corresponding activation barriers for the insertion process are 17.3 and 21.2 kcal·mol^{-1}, respectively. The energy difference of almost 4.0 kcal·mol^{-1} between the activation barriers highlights the kinetic preference for the hydride (denoted as H^1) to migrate at the carbon (denoted as C^a) bearing the cyclic amine group (Figure 6). The associated intermediates (according to IRC calculations) of this process lie at 1.5 and 2.3 kcal·mol^{-1} with respect to the initial complex **E2**, leading to an endoergic step by 6.9 and 7.7 kcal·mol^{-1}, respectively. Intermediate **E4a** adopts geometry closer to a tetrahedral one, in contrast with **E4b**, which adopts an almost square planar geometry. It should be noted that all attempts to locate an intermediate in which a secondary interaction between the nitrogen and the rhodium exists failed, ruling out any possible existence of such a species on the potential energy surface, in contrast to related computational studies.[15] This can be attributed to the different type of phosphine that is used in the latter studies (triphenylphosphine) rather than the rigid chelating one, which is used in the present work. The following process in the reaction sequence corresponds to the coordination of H_2 to form a dihydrogen intermediate and the subsequent oxidative addition of the latter to form the dihydrido species. The coordination of H_2 is endoergic for both pathways (10.9 and 18.4 kcal·mol^{-1}, respectively, due to entropy loss upon coordination) while the oxidative addition corresponds to a barrierless process. The corresponding complexes adopt an octahedral geometry, with the hydride and the carbonyl group lying in the axial positions. It should be noted that the oxidative addition of dihydrogen is an endergonic process in both cases (3.7 and 9.3 kcal·mol^{-1}, respectively), being in line with a previous joined experimental/theoretical study on catalytic hydrogenation of enamides using cationic complexes of rhodium.[43] Finally, in the last step, migration of a hydride to the alkylamine takes place, allowing the formation of the *S*-product along with catalyst regeneration. From each of the two intermediates **E6a** and **E6b**, there are two possibilities for the final hydrogenation of the alkylamine, as shown in the Gibbs free energy reaction profile in Figure 6. Indeed, from intermediate **E6a** the reductive elimination of the final product can be achieved either via $\mathbf{TS_{E6a\text{-}E2'}}$ or $\mathbf{TS_{E6a\text{-}E2}}$, overcoming an activation barrier of 15.2 or 13.2 kcal·mol^{-1}, respectively. The first case corresponds to the migration of the axial hydride (H^2 in Figure 6), while in the second one, corresponds to the migration of the equatorial hydride (H^3) to the alkylamine group. The energy difference between these transition states is 2.0 kcal·mol^{-1} in favor of $\mathbf{TS_{E6a\text{-}E2}}$. While the outcome of $\mathbf{TS_{E6a\text{-}E2}}$ is directly **E2** along with the formation of the *S*-product, in contrast $\mathbf{TS_{E6a\text{-}E2'}}$ gives the relatively unstable intermediate **E2′** and *S*-product, which upon isomerization forms the active catalyst **E2**. A similar situation applies in the case of intermediate **E6b**. The corresponding activation barriers are lower than in previous case by almost 11 kcal·mol^{-1}. This can be explained by the energy difference between intermediates **E6a** and **E6b** (6.4 kcal·mol^{-1} in favor of **E6a**) and the kinetic preference for the migration of hydride to the

dx.doi.org/10.1021/cs400906b | ACS Catal. 2014, 4, 435−447

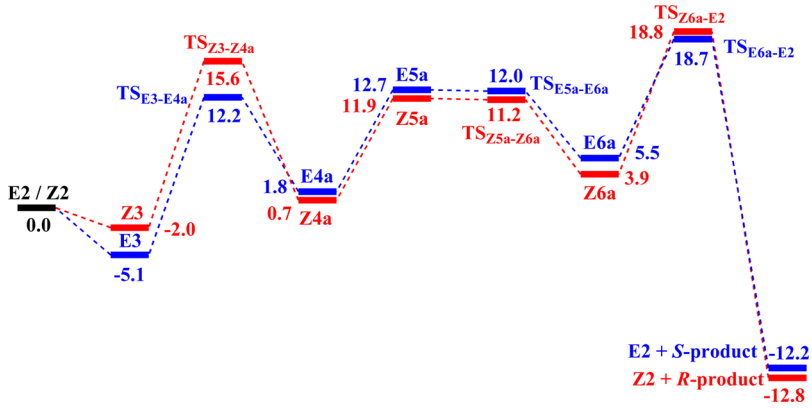

Figure 8. Comparison between the two most favorable pathways for (*E*)- and (*Z*)-enamine cases (in kcal·mol^{-1}).

C^a over C^b (3.9 kcal·mol^{-1}, leading to a difference of 10.3 kcal·mol^{-1}). Overall, the catalytic reaction is found to be exoergic by −12.5 kcal·mol^{-1}.

The same mechanistic scenario applies in the case of *Z*-enamine, as depicted in Figure 7, and is very similar to the (*E*)-case.

The only difference occurs in the reductive elimination step. Indeed, the energetic stability of the two intermediates (**Z6a** and **Z6b**) matches the energy ordering of the four corresponding transition states (no energetic crossing is observed). Thus, the general energetic trend is maintained for all the stationary points of the pathways. In addition, it is worth noting that the energy gap between the two transition states of the insertion step decreases substantially with respect to the analogues in the (*E*)-enamine case (1.1 vs 3.9 kcal·mol^{-1}). Finally, while the pathway corresponding to (*E*)-enamine leads to the (*S*)-product, the (*Z*)-enamine one gives the (*R*)-product. In order to shed light to the experimental observed lack of enantioselectivity of the reaction when a racemic mixture of enamine is used, a comparison between the two most energetically favorable corresponding pathways is required and displayed in Figure 8.

It should be noted that in order to make the direct comparison between the two isomers, we had to shift all the values of the (*E*)-enamine pathway by 0.3 kcal·mol^{-1}. The latter value corresponds to the energy difference between the two organic isomers, in favor of (*Z*)-enamine. Perusal of Figure 8 reveals that both pathways almost overlap. First, the highest activation barrier for (*E*)-enamine pathway is 17.3 kcal·mol^{-1} being very close to the analogous case for (*Z*)-enamine, with the latter being 17.6 kcal·mol^{-1}, both corresponding to the hydride migration. This is the rate-limiting step of the mechanism, as already pointed out in previous theoretical works on hydride transfer on alkenes.[44] More importantly for the catalytic activity, the highest point in both pathways corresponds to the final reductive elimination transition state, being identical in terms of energy (∼18.8 kcal·mol^{-1} with respect to **E2**). It should be noted that reaction profiles starting from other enamine adducts (different enantiofaces coordinated, namely **E3-rot-ef** and **Z3-ef**, see SI, Figures S6 and S7) involve much higher relative energy for the reductive elimination step (more than 22.7 kcal·mol^{-1}) than those reported above and are thus not competitive. In terms of thermodynamics, both pathways have overall the same energy (−12.2 and −12.8 kcal·mol^{-1} for (*E*)- and (*Z*)-enamine case, respectively). On the basis of the aforesaid theoretical observations and taking into account the DFT error, which is in general in the range of ±2 kcal·mol^{-1}, all profiles can be considered as equivalent in energy, and these considerations explain the lack of enantiomeric excess observed experimentally when using this particular catalytic system.

CONCLUSION

In this study, we have analyzed the rhodium-catalyzed HAM reaction involving mainly styrene and piperidine. Among the considered chiral diphosphine ligands, the diphospholane ligands allow reaching a higher reaction rate and selectivity in 1-(2-phenylpropyl)piperidine. The reactivity of both neutral [Rh(acac)(CO)$_2$]/diphosphine and cationic [Rh(CO)$_2$(P−P)]$^+$ systems have been studied. The catalytic results and HP NMR data show that although the neutral complex [RhHCO)$_2$(P−P)], considered to be the precursor of the active species for both hydroformylation and hydrogenation reactions, can be formed from either the neutral or cationic precursors, it is the neutral [Rh(acac)(CO)$_2$]/diphosphine system that is the more efficient, probably due to a higher concentration in the active species. This result highlights that under HAM conditions (presence of CO/H$_2$ and amine), the catalytic activity of a given system cannot be easily anticipated only on the basis of the intrinsic activity for hydroformylation and hydrogenation.

A surprising result of this study is the complete lack of enantioselectivity, whatever the {rhodium−chiral ligand} system involved. Catalytic experiments have shown that a mixture of (*Z*) and (*E*)-enamines is produced during the one-pot reaction. DFT calculations revealed that the formation of the [RhHCO(P−P)] active species from the [RhH(CO)$_2$(P−P)] precursor is energy demanding (18.7 kcal·mol^{-1}). From this active species, the rate-determining-step of the HAM is the migration of a hydride to the alkylamine ligand. The pathways for the (*E*)- and (*Z*)-enamine cases have overall the same energy (−12.2 and −12.8 kcal·mol^{-1}), explaining the lack of enantioselectivity in the present case. Hydroaminomethylation is a complex tandem reaction, and this study constitutes the first attempt of an asymmetric one-pot reported version of this reaction. Although our results show the absence of enantioselectivity for a given system, we believe that additional efforts should be devoted. As far as the catalytic system is concerned, the use of larger bite-angle diphosphines might orientate the enamine coordination mode and change the energy difference between the transitions states. Another couple of amine/alkene starting substrates might also favor

dx.doi.org/10.1021/cs400906b | *ACS Catal.* 2014, 4, 435−447

the formation of only one enamine isomer and its coordination in an enantiofacial discrimination mode. This study shed light on catalytic species involved in the reaction and opens new perspectives for further investigations on this challenging reaction.

EXPERIMENTAL SECTION

General Considerations. All NMR spectra data were recorded on Bruker DRX 300 or Avance 300−500 spectrometers with TMS as internal reference for ^{1}H and ^{13}C, 85% phosphoric acid as external reference for ^{31}P. Chemical shifts are reported in ppm, and coupling constants (J) are given in Hertz. All experiments were carried out under argon using Schlenk techniques or glovebox. Solvents were obtained from a Solvent Purification System (MB SPS-800) or were previously distilled. Rhodium complexes were prepared according to previously described procedures.[16,17] Products were characterized by gas chromatography (GC, chiral GC, and GC-MS) and NMR (see SI).

General Procedure for Hydroaminomethylation Experiments. All experiments were performed following the same procedure in a 90 mL stainless-steel autoclave purchased from TOP Industrie. The gas mixture was previously prepared in the desired pCO/pH_2 ratio. The alkene (10 mmol) and the amine (10 mmol) were introduced in the reactor, followed by the rhodium complex and the ligand solubilized in the solvent. The closed reactor was then purged three times with the CO/H_2 gas mixture. The reaction mixture was placed under 10 bar CO/H_2 and heated until the desired temperature with a 1000 rpm stirring rate. The pressure was then completed until 30 bar CO/H_2. The experiment was running under a continuous feed of gas mixture. Samples were taken during the experiment in order to follow the reaction course by gas chromatography (see SI) or NMR. The autoclave was cooled to room temperature and then slowly depressurized. The crude mixture was analyzed by gas chromatography.

HP-NMR Spectroscopic Studies. A 10 mm sapphire tube was charged under argon with 1.5 mL of deuterated solvent solution of the rhodium complex (0.025 mmol) and then with amine or and alkene. $^{31}P\{1H\}$and ^{1}H NMR spectra of the solution were acquired at 298 K. Then, the NMR tube was charged with 30 bar of CO/H_2 (1:2), and further HP-NMR spectra were recorded at room temperature or under heating, according to the experiments carried out.

COMPUTATIONAL METHODS

All calculations were performed with the Gaussian09 package[45] of programs. To take into account any possible weak dispersion interactions in the catalytic system under study, the pure GGA functional B97D was used, which contains the corresponding dispersion empirical correction in its formulation.[46] The Rh and P atoms were represented by the relativistic effective core potential (RECP) from the Stuttgart group and the associated basis sets[47,48] augmented by a f (α = 1.350)[49] and d (α = 0.387)[50] polarization functions, respectively. The remaining nonmetal atoms were represented by a 6-31G(d,p) basis set.[51] Gibbs free energies were obtained at T = 298.15K within the harmonic approximation. In all computations, no constraints were imposed on the geometry. Intrinsic Reaction Paths (IRPs)[52] were traced from the various transition structures to verify the reactant to product linkage. Finally, the CYL view program was used for the representation of 3D structures.[53]

ASSOCIATED CONTENT

Supporting Information

Text, tables for experimental details, and DFT calculations data. This material is available free of charge via the Internet at http://pubs.acs.org.

AUTHOR INFORMATION

Corresponding Authors

*E-mail: philippe.kalck@ensiacet.fr.
*E-mail: martine.urrutigoity@ensiacet.fr.
*E-mail: laurent.maron@irsamc.ups-tlse.fr.

Notes

The authors declare no competing financial interest.

ACKNOWLEDGMENTS

L.M. is a member of the Institut Universitaire de France. CALMIP and CINES are acknowledged for generously granting computing time. L.M. would like to thank the Humboldt Foundation. The authors thank CNRS and UPS for the financial support of this work. Pr. Carmen Claver and her group are gratefully acknowledged for the opportunity given to perform some HP NMR experiments and for fruitful discussions.

REFERENCES

(1) (a) March, J., *Advanced Organic Chemistry*, 4th ed.; Wiley-Interscience: New York, 1992; pp 768 and references therein; (b) Heilen, G., Mercker, H. J., Frank, D., Reck, A., Jäckh, R. *Ullmanns Encyclopedia of Industrial Chemistry*; Wiley-VCH: Weinheim, Germany, 1985; Vol. *A2*, p 1.

(2) (a) Blunt, J. W.; Copp, B. R.; Keyzers, R. A.; Munro, M. H. G.; Prinsep, M. R. *Nat. Prod. Rep.* **2012**, *29*, 144−122. (b) Blunt, J. W.; Copp, B. R.; Munro, M. H. G.; Northcote, P. T.; Prinsep, M. R. *Nat. Prod. Rep.* **2009**, *26*, 170−237.

(3) (a) *Applied Homogeneous Catalysis with Organometallic Compounds*, 2nd ed.; Cornils, B., Herrmann, W. A., Eds.; Wiley-VCH: Weinheim, Germany; 2002. (b) *Green Chemistry and Catalysis*; Sheldon, R. A., Arends, I., Hanefeld, U., Eds.; Wiley-VCH: Weinheim, Germany, 2007.

(4) (a) Eilbracht, P.; Bärfacker, L.; Buss, C.; Hollmann, C.; Kitsos-Rzychon, B. E.; Kranemann, C. L.; Rische, T.; Roggenbuck, R.; Schmidt, A. *Chem. Rev.* **1999**, *99*, 3329−3365. (b) Eilbracht, P., Schmidt, A. M. In *Transition Metals for Organic Synthesis*, 2nd ed.; Beller, M., Bolm, C., Eds.; Wiley-VCH: Weinheim, Germany, 2004; Vol. *1*, pp 57−85. (c) Eilbracht, P.; Schmidt, A. M. *Top. Organomet. Chem.* **2006**, *18*, 65−95. (d) Crozet, D.; Urrutigoïty, M.; Kalck, P. *ChemCatChem* **2011**, *3*, 1102−1118.

(5) Fogg, D. E.; dos Santos, E. N. *Coord. Chem . Rev.* **2004**, *248*, 2365−2379.

(6) *Rhodium Catalyzed Hydroformylation*; van Leeuwen, P.W.N.M., Claver, C., Eds.; Kluwer Academic Publishers: The Netherlands, 2000.

(7) Kamer, P. C. J.; Reek, J. N. H., van Leeuwen, P.W.N.M. In *Mechanisms in Homogeneous Catalysis. A Spectroscopic Approach.*; Heaton, B., Ed.; Wiley-VCH: Weinheim, Germany, 2005; pp 231−270.

(8) Oro, L. A.; Carmona, D. In *The Handbook of Homogeneous Hydrogenation*; de Vries, J. G., Elsevier, C. J., Eds.; Wiley-VCH: Weinheim, Germany, 2007; Vol. *1*, pp 3−30.

(9) Giernoth, R. In *Mechanisms in Homogeneous Catalysis. A Spectroscopic Approach.* Heaton, B., Ed.; Wiley-VCH: Weinheim, Germany, 2005; pp 359−378.

(10) (a) Pamies, O.; Net, G.; Widhalm, M.; Ruiz, A.; Claver, C. *J. Organomet. Chem.* **1999**, *587*, 136−143. (b) Orejón, A.; Masdeu-Bultó, A. M.; Echarri, R.; Diéguez, M.; Forniés-Cámer, J.; Claver, C.; Cardin, C. J. *J. Organomet. Chem.* **1998**, *559*, 23−29. (c) Rosales, M.; González, A.; Guerrero, Y.; Pacheco, I.; Sánchez-Delgado, R. A. *J. Mol. Catal. A:*

Chem. **2007**, *270*, 241−249. (d) Rosales, M.; Durán, J. A.; González, A.; Pacheco, I.; Sánchez-Delgado, R. A. *J. Mol. Catal. A: Chem.* **2007**, *270*, 250−256. (e) Zhou, Z.; Facey, G.; James, B. R.; Alper, H. *Organometallics* **1996**, *15*, 2496−2503.
(11) Noonan, G. M.; Newton, D.; Cobley, C. J.; Suarez, A.; Pizzano, A.; Clarke, M. L. *Adv. Synth. Catal.* **2010**, *352*, 1047−1054.
(12) (a) Rische, T.; Kitsos-Rzychon, B.; Eilbracht, P. *Tetrahedron* **1998**, *54*, 2723−2742. (b) Rische, T.; Eilbracht, P. *Synthesis* **1997**, 1331−1337.
(13) Lin, Y.-S.; El Ali, B.; Alper, H. *Tetrahedron Lett.* **2001**, *42*, 2423−2425.
(14) Routaboul, L.; Buch, C.; Klein, H.; Jackstell, R.; Beller, M. *Tetrahedron Lett.* **2005**, *46*, 7401−7405.
(15) Fuentes, J. A.; Wawrzyniak, P.; Roff, G. J.; Bühl, M.; Clarke, M. L. *Catal. Sci. Technol.* **2011**, *1*, 431−436.
(16) Crozet, D.; Gual, A.; McKay, D.; Dinoi, C.; Godard, C.; Urrutigoïty, M.; Daran, J.-C.; Maron, L.; Claver, C.; Kalck, P. *Chem.—Eur. J.* **2012**, *18*, 7128−7140.
(17) Crozet, D.; McKay, D.; Bijani, C.; Gual, A.; Godard, C.; Claver, C.; Maron, L.; Urrutigoïty, M.; Kalck, P. *Dalton Trans.* **2012**, *41*, 3369−3373.
(18) (a) Clarke, M. L.; Ellis, D.; Mason, K. L.; Orpen, A. G.; Pringle, P. G.; Wingad, R. L.; Zaher, D. A.; Baker, R. T. *Dalton Trans.* **2005**, 1294−1300. (b) van der Slot, S.; Duran, J.; Luten, J.; Kamer, P. C. J.; van Leeuwen, P. W. N. M. *Organometallics* **2002**, *21*, 3873−3883.
(19) (a) Nozaki, K., Ojima, I. In *Catalytic Asymmetric Synthesis*, 2nd ed.; Ojima, I., Ed.; Wiley-VCH: New York, 2000; p 429. (b) Godard, C.; Ruiz, A.; Diéguez, M.; Pàmies, O.; Claver, C. In *Catalytic Asymmetric Synthesis*, 3rd ed.; Ojima, I., Ed.; Wiley: New York, 2010; pp799−838.
(20) (a) Brown, J. M. In *The Handbook of Homogeneous Hydrogenation*; de Vries, J. G., Elsevier, C. J., Eds.; Wiley-VCH: Weinheim, Germany, 2007; Vol. *1*, pp 1073−1104.
(21) (a) Halpern, J.; Riley, D. P.; Chan, A. S. C.; Pluth, J. J. *J. Am. Chem. Soc.* **1977**, *99*, 8055−8057. (b) Chan, A. S. C.; Halpern, J. *J. Am. Chem. Soc.* **1980**, *102*, 838−840. (c) Landis, C. R.; Halpern, J. *J. Am. Chem. Soc.* **1987**, *109*, 1746−1754.
(22) (a) Klosin, J.; Landis, C. R. *Acc. Chem. Res.* **2007**, *40*, 1251−1259. (b) Axtell, A. T.; Klosin, J.; Abboud, K. A. *Organometallics* **2006**, *25*, 5003−5009. (c) Clark, T. P.; Landis, C. R. *Tetrahedron: Asymm.* **2004**, *15*, 2123−2137.
(23) Zhang, W.; Chi, Y.; Zhang, X. *Acc. Chem. Res.* **2007**, *40*, 1278−1290.
(24) Shang, G., Zhang, X. In *Phosphorus Ligands in Asymmetric Catalysis, Synthesis and Applications* (Ed: Börner, A., Eds.; Wiley-VCH: Weinheim, Germany, 2008; pp 135−205.
(25) (a) Pilkington, C. J.; Zanotti-Gerosa, A. *Org. Lett.* **2003**, *5*, 1273−1275. (b) Harrison, P.; Meek, G. *Tetrahedron Lett.* **2004**, *45*, 9277−92802.
(26) (a) Burk, M. J.; Bienewald, F.; Harris, M.; Zanotti-Gerosa, A. *Angew. Chem., Int. Ed.* **1998**, *37*, 1931−1933. (b) Burk, M. J.; Wang, Y. M.; Lee, J. R. *J. Am. Chem. Soc.* **1996**, *118*, 5142−5143. (c) Burk, M. J.; Gross, M. F.; Martinez, J. P. *J. Am. Chem. Soc.* **1995**, *117*, 9375−9376.
(27) Axtell, A. T.; Cobley, C. J.; Klosin, J.; Whiteker, G. T.; Zanotti-Gerosa, A.; Abboud, K. A. *Angew. Chem., Int. Ed.* **2005**, *44*, 5834−5838.
(28) (a) Tang, W.; Zhang, X. *Angew. Chem., Int. Ed.* **2002**, *41*, 1612−1614. (b) Zhang X., Tang W. Penn State Research Institute, WO 03/042135, 2003.
(29) (a) Liu, D.; Zhang, X. *Eur. J. Org. Chem.* **2005**, 646−649. (b) Zhang X., Tang W. Penn State Research Foundation, US 2004/0229846 A1, 2004.
(30) Tang, W.; Wang, W.; Chi, Y.; Zhang, X. *Angew.Chem., Int. Ed.* **2003**, *42*, 3509−3511.
(31) (a) Tang, W.; Zhang, X. *Angew. Chem., Int. Ed.* **2002**, *41*, 1612−1614. (b) Yang, Q.; Shang, G.; Gao, W.; Deng, J.; Zhang, X. *Angew. Chem., Int. Ed.* **2006**, *45*, 3832−3835. (c) Shang, G.; Yang, Q.; Zhang, X. *Angew. Chem., Int. Ed.* **2006**, *45*, 6360−6362. (d) Sun, X.; Zhou, L.; Wang, C.-J.; Zhang, X. *Angew. Chem., Int. Ed.* **2007**, *46*, 2623−2626.
(e) Tang, W.; Zhang, X. *Org. Lett.* **2002**, *4*, 4159−416. (f) Huang, J.; Bunel, E.; Allgeier, A.; Tedrow, J.; Storz, T.; Preston, J.; Correll, T.; Manley, D.; Soukup, T.; Jensen, R.; Syed, R.; Moniz, G.; Larsen, R.; Martinelli, M.; Reider, P. J. *Tetrahedron Lett.* **2005**, *46*, 7831−7834.
(32) Shimizu, H.; Nagasaki, I.; Sayo, N.; Saito, T. In *Phosphorus Ligands in Asymmetric Catalysis*; Börner, A., Ed.; Wiley-VCH: Weinheim, Germany, 2008; pp 207−260.
(33) Schmid, R.; Foricher, J.; Cereghetti, M.; Schoenholzer, P. *Helv. Chim. Acta* **1991**, *74*, 370−89.
(34) Duprat de Paule, S.; Jeulin, S.; Ratovelomanana-Vidal, V.; Genêt, J.-P.; Champion, N.; Dellis, P. *Eur. J. Org. Chem.* **2003**, 1931−1941.
(35) Blaser, H.-U.; Brieden, W.; Pugin, B.; Spindler, F.; Studer, M.; Togni, A. *Topics Catal.* **2002**, *19*, 3−16.
(36) (a) Seayad, A.; Ahmed, M.; Klein, H.; Jackstell, R.; Gross, T.; Beller, M. *Science* **2002**, *297*, 1676−1678. (b) Ahmed, M.; Seayad, A.; Jackstell, R.; Beller, M. *J. Am. Chem. Soc.* **2003**, *125*, 10311−10318. (c) Ahmed, M.; Bronger, R. P. J.; Jackstell, R.; Kamer, P. C. J.; van Leeuwen, P. W. N. M.; Beller, M. *Chem.—Eur. J.* **2006**, *12*, 8979−8988.
(37) Hamers, B.; Kosciusko-Morizet, E.; Müller, C.; Vogt, D. *ChemCatChem* **2009**, *1*, 103−106.
(38) Hamers, B.; Bäuerlin, P. S.; Müller, C.; Vogt, D. *Adv. Synth. Catal.* **2008**, *350*, 332−342.
(39) (a) Zhang, W.; Chi, Y.; Zhang, X. *Acc. Chem. Res.* **2007**, *40*, 1278−1290. (b) Tang, W.; Zhang, X. *Angew. Chem., Int. Ed.* **2002**, *41*, 1612−1614. (c) Tang, W.; Wang, W.; Chi, Y.; Zhang, X. *Angew. Chem., Int. Ed.* **2003**, *42*, 3509−3511.
(40) (a) Scheuermann, C. J.; Jaekel, C. *Adv. Synth. Catal.* **2008**, *350*, 2708−2714. (b) Jäkel, C.; Paciello, R. In *Asymmetric Catalysis on Industrial Scale, Chalenges, Approaches and Solutions*, 2nd ed.; Blaser, H.-U., Federsel, H.-J., Eds.; Wiley-VCH: Weinheim, Germany, 2010; pp 187−205.
(41) Rosales, M.; Gonzalez, A.; Guerrero, Y.; Pacheco, I.; Sanchez-Delgado, R. A. *J. Mol. Cat. A: Chem.* **2007**, *270*, 241−249.
(42) Scheuermann, C. J.; Jaekel, C. *Adv. Synth. Catal.* **2008**, *350*, 2708−2714.
(43) Landis, C. R.; Hilfenhaus, P.; Feldgus, S. *J. Am. Chem. Soc.* **1999**, *121*, 8741−8754.
(44) Nelson, D. J.; Li, R.; Brammer, C. *J. Org. Chem.* **2005**, *70*, 761−767.
(45) Frisch, M. J.; Trucks, G. W.; Schlegel, H. B.; Scuseria, G. E.; Robb, M. A.; Cheeseman, J. R.; Scalmani, G.; Barone, V.; Mennucci, B.; Petersson, G. A.; Nakatsuji, H.; Caricato, M.; Li, X.; Hratchian, H. P.; Izmaylov, A. F.; Bloino, J.; Zheng, G.; Sonnenberg, J. L.; Hada, M.; Ehara, M.; Toyota, K.; Fukuda, R.; Hasegawa, J.; Ishida, M.; Nakajima, T.; Honda, Y.; Kitao, O.; Nakai, H.; Vreven, T.; Montgomery, Jr., J. A.; Peralta, J. E.; Ogliaro, F.; Bearpark, M.; Heyd, J. J.; Brothers, E.; Kudin, K. N.; Staroverov, V. N.; Kobayashi, R.; Normand, J.; Raghavachari, K.; Rendell, A.; Burant, J. C.; Iyengar, S. S.; Tomasi, J.; Cossi, M.; Rega, N.; Millam, J. M.; Klene, M.; Knox, J. E.; Cross, J. B.; Bakken, V.; Adamo, C.; Jaramillo, J.; Gomperts, R.; Stratmann, R. E.; Yazyev, O.; Austin, A. J.; Cammi, R.; Pomelli, C.; Ochterski, J. W.; Martin, R. L.; Morokuma, K.; Zakrzewski, V. G.; Voth, G. A.; Salvador, P.; Dannenberg, J. J.; Dapprich, S.; Daniels, A. D.; Farkas, Ö.; Foresman, J. B.; Ortiz, J. V.; Cioslowski, J.; Fox, D. J. *Gaussian 09*, revision A.02; Gaussian, Inc., Wallingford CT, 2009.
(46) Grimme, S. *J. Comput. Chem.* **2006**, *27*, 1787.
(47) Andrae, D.; Haussermann, U.; Dolg, M.; Stoll, H.; Preuss, H. *Theor. Chim. Acta* **1990**, *77*, 123.
(48) Bergner, A.; Dolg, M.; Kuchle, W.; Stoll, H.; Preuss, H. *Mol. Phys.* **1993**, *30*, 1431.
(49) Ehlers, A. W.; Bohme, H.; Dapprich, S.; Gobbi, A.; Hollwarth, A.; Jonas, V.; Kohler, K. F.; Stegmann, R.; Veldkamp, A.; Frenking, G. *Chem. Phys. Lett.* **1993**, *203*, 111.
(50) Hollwarth, A.; Bohme, H.; Dapprich, S.; Ehlers, A. W.; Gobbi, A.; Jonas, V.; Kohler, K. F.; Stegmann, R.; Veldkamp, A.; Frenking, G. *Chem. Phys. Lett.* **1993**, *203*, 237.
(51) Hariharan, P. C.; Pople, J. A. *Theor. Chim. Acta* **1973**, *28*, 213.

(52) (a) Gonzalez, C.; Schlegel, H. B. *J. Chem. Phys.* **1989**, *90*, 2154−2161. (b) Gonzalez, C.; Schlegel, H. B. *J. Phys. Chem.* **1990**, *94*, 5523−5527.
(53) Legault, C. Y. CYLview, version 1.0b. Université de Sherbrooke, 2009. http://www.cylview.org.

■ NOTE ADDED AFTER ASAP PUBLICATION

This paper was published on the Web on January 6, 2014. The Abstract graphic was revised, and minor changes made to the footnotes of Table 1, and the paper was reposted on January 9, 2014. An error in the title of the paper was discovered, and the paper was reposted on January 13, 2014.